Supporting information

for

Highly cytotoxic gold(I)-phosphane dithiocarbamate complexes trigger an ER stress-dependent immune response in ovarian cancer cells

Hai Van Le,[a, ≠] Maria V. Babak,[a, ≠] Muhammad Ali Ehsan,[b]‡ Muhammad Altaf,[b,c] Lisa Reichert,[a] Artem L. Gushchin,[d,e] Wee Han Ang,[a,f]* Anvarhusein A. Isab[g]*

[a]Department of Chemistry, National University of Singapore, 3 Science Drive 2, 117543 Singapore
[b]Center of Research Excellence in Nanotechnology, King Fahd University of Petroleum & Minerals, Dhahran 31261, Saudi Arabia
[c]Department of Chemistry, Government University College Lahore, Pakistan
[d]Nikolaev Institute of Inorganic Chemistry, Siberian Branch of Russian Academy of Sciences, 3 Acad. Lavrentiev Avenue, Novosibirsk 630090, Russia
[e]Novosibirsk State University, 2 Pirogov Street, 630090 Novosibirsk, Russia
[f]NUS Graduate School for Integrative Sciences and Engineering, Singapore; e-mail: chmawh@nus.edu.sg
[g] Department of Chemistry, King Fahd University of Petroleum and Minerals, Dhahran 31261, Saudi Arabia;
≠ Both authors contributed equally to this manuscript
e-mail: aisab@kfupm.edu.sa

Table S1. Crystal data and details of data collection for **1**, **2′**, **3** and **4**.

Table S2. Key bond lengths and angles observed in the molecular structures of **1**, **3** and **4**.

Table S3. Cytotoxicity of complex **2**, auranofin and cDDP in presence or absence of antioxidants.

Figure S1. ^{1}H NMR (top) and ^{31}P NMR (bottom) spectra of **1** in pyridine-d^{5}.

Figure S2. ^{1}H NMR (top) and ^{31}P NMR (bottom) spectra of **2** in pyridine-d^{5}.

Figure S3. ^{1}H NMR spectra of **2** in DMSO-d^{6} immediately after dissolution and 10 d after dissolution.

Figure S4. ^{1}H NMR (top) and ^{31}P NMR (bottom) spectra of **3** in $CDCl_3$ immediately after dissolution.

Figure S5. ^{1}H NMR (top) and ^{31}P NMR (bottom) spectra of **4** in MeOH-d^{4} immediately after dissolution.

Figure S6. ^{1}H NMR spectra of **4** in DMSO-d^{6} immediately after dissolution (top) and 5 min, 4 h and 14 d after dissolution (bottom).

Figure S7. High resolution EI-MS spectrum of **1**.

Figure S8. High resolution EI-MS spectrum of **2**.

Figure S9. High resolution EI-MS spectrum of **3**.

Figure S10. High resolution EI-MS spectrum of **4**.

Figure S11. FT-IR spectra of **1**-**4**.

Figure S12. Molecular structure of **4.**

Figure S13. Concentration-effect curves of **1**-**4**, auranofin and cDDP in the human ovarian carcinoma cell lines A2780 and A2780cis obtained by the MTT assay using exposure times of 72 h.

Figure S14. Concentration-effect curves of **2** and cDDP in the human ovarian carcinoma cell line A2780 obtained by the MTT assay using exposure times of 24 h in presence or absence of antioxidants.

Figure S15. Cell cycle analysis of A2780 cells treated with **2**, auranofin and cisplatin for 24 h.

Table S1. Crystal data and details of data collection for **1**, **2′**, **3**, **4**.

Complex	**1**	**2′**	**3**	**4**
CCDC number	1996351	1996352	1996353	1996354
Empirical formula	$C_{23.50}H_{34}AuClNPS_2$	$C_{40.50}H_{81}Au_8C_lN_8S_{16}$	$C_{27}H_{41}AuNPS_2$	$C_{29}H_{45}AuNPS_2$
Fw	658.02	2804.27	671.66	699.71
Crystal system	monoclinic	orthorhombic	monoclinic	triclinic
Space group	*C*2/*c*	*Fdd*2	$P2_1/c$	$P\bar{1}$
a, Å	35.3443(12)	26.0916(10)	10.9925(4)	9.5931(2)
b, Å	11.0755(4)	44.773(2)	13.0068(4)	11.3803(3)
c, Å	30.2179(11)	24.5430(10)	19.4730(6)	15.1080(3)
α, deg	90	90	90	107.692(1)
β, deg	118.915(1)	90	97.2120(13)	104.572(1)
γ, deg	90	90	90	96.872(1)
V, $Å^3$	10354.4(6)	28671(2)	2762.17(16)	1486.02(6)
Z	16	16	4	2
λ, Å	0.71073	0.71073	0.71073	0.71073
ρ_{calcd}, g cm^{-3}	1.688	2.599	1.615	1.564
Crystal size, mm^3	0.477 x 0.250 x 0.226	0.097 x 0.083 x 0.043	0.487 x 0.236 x 0.104	0.338 x 0.180 x 0.126
T, K	100(2)	100(2)	100(2)	100(2)
μ, cm^{-1}	60.21	168.45	55.51	51.62
Reflns collected/unique	50858	185714	26804	30790
[R_{int}]	0.0309	0.0923	0.0288	0.0313
$R1^a$	0.0231	0.0284	0.0248	0.0174
$wR2^b$	0.0475	0.0434	0.0583	0.0380
GOF^c	1.065	1.021	1.118	1.059

[a] $R_1 = \Sigma||Fo| - Fc||/\Sigma|Fo|$

[b] $wR2 = \{\Sigma w(Fo^2 - Fc^2)^2/\Sigma w(Fo^2)^2\}^{1/2}$

[c] $GOF = \{\Sigma[w(Fo^2 - Fc^2)^2]/(n-p)^{1/2}$, where *n* is the number of reflections and *p* is the total number of parameters refined.

Table S2. Key bond lengths and angles observed in the molecular structures of **1**, **3** and **4**.

Bond lengths (Å) and angles (°)	**Compound**		
	1	**3**	**4**
CCDC number	1996351	1996353	1996354
Au1-P1 / Å	2.2710(7)	2.2688(7)	2.2677(5)
Au1-S1 / Å	2.3202(7)	2.3344(8)	2.3415(5)
C7-C8 / Å	1.400(4)	1.401(4)	1.404(3)
C7-C12 / Å	1.409(4)	1.412(4)	1.412(3)
C8-C9 / Å	1.385(4)	1.375(5)	1.376(3)
C9-C10 / Å	1.388(4)	1.375(5)	1.387(3)
C10-C11 / Å	1.383(4)	1.392(4)	1.386(3)
C11-C12 / Å	1.407(4)	1.405(4)	1.402(3)
P1-C12 / Å	1.835(3)	1.834(3)	1.837(2)
P1-C13 / Å	1.883(3)	1.889(3)	1.887(2)
P1-C17 / Å	1.884(3)	1.890(3)	1.880(2)
S1-C21 / Å	1.758(3)	1.745(3)	1.744(2)
S2-C21 / Å	1.686(3)	1.699(3)	1.693(2)
N1-C21 / Å	1.342(3)	1.332(4)	1.353(3)
N1-C22 / Å	1.449(4)	1.447(5)	1.476(3)
N1-C23 / Å	1.461(4)	1.564(5)	1.474(3)
P1-Au1-S1 / °	174.99(3)	171.37(3)	172.967(18)
C21-S1-Au1 / °	101.38(9)	98.92(11)	98.18(7)
C12-P1-Au1 / °	116.06(8)	106.36(10)	114.91(7)
C7-C12-P1 / °	122.82(19)	123.0(2)	122.70(15)
C11-C12-P1 / °	119.0(2)	119.1(2)	118.85(15)
S2-C21-S1 / °	122.03(16)	118.20(19)	119.33(12)
N1-C21-S1 / °	115.8(2)	120.4(3)	118.08(16)
N1-C21-S2 / °	122.1(2)	121.5(3)	122.58(16)
C21-N1-C22 / °	122.9(2)	130.4(4)	120.20(18)
C21-N1-C23 / °	122.9(2)	116.7(3)	123.06(18)
C23-N1-C22 / °	114.1(2)	112.8(3)	115.52(18)

Table S3. Cytotoxicity of **2**, auranofin and cDDP in presence or absence of antioxidants (NAC – *N*-acetyl cysteine, KI – potassium iodide, AA – acetic acid)

	IC_{50} [nm][a]			
Compound	**No antioxidants**	**NAC**	**KI**	**AA**
2	49 ± 16	113 ± 42	48 ± 12	33 ± 7
cisplatin	7867 ± 1444	10827 ± 380	8906 ± 1207	6826 ± 2796

[a] 50% inhibitory concentrations in A2780 cells determined by MTT assay after 2 h pre-incubation with respective antioxidants and 24 h co-incubation with **2**, auranofin and cDDP

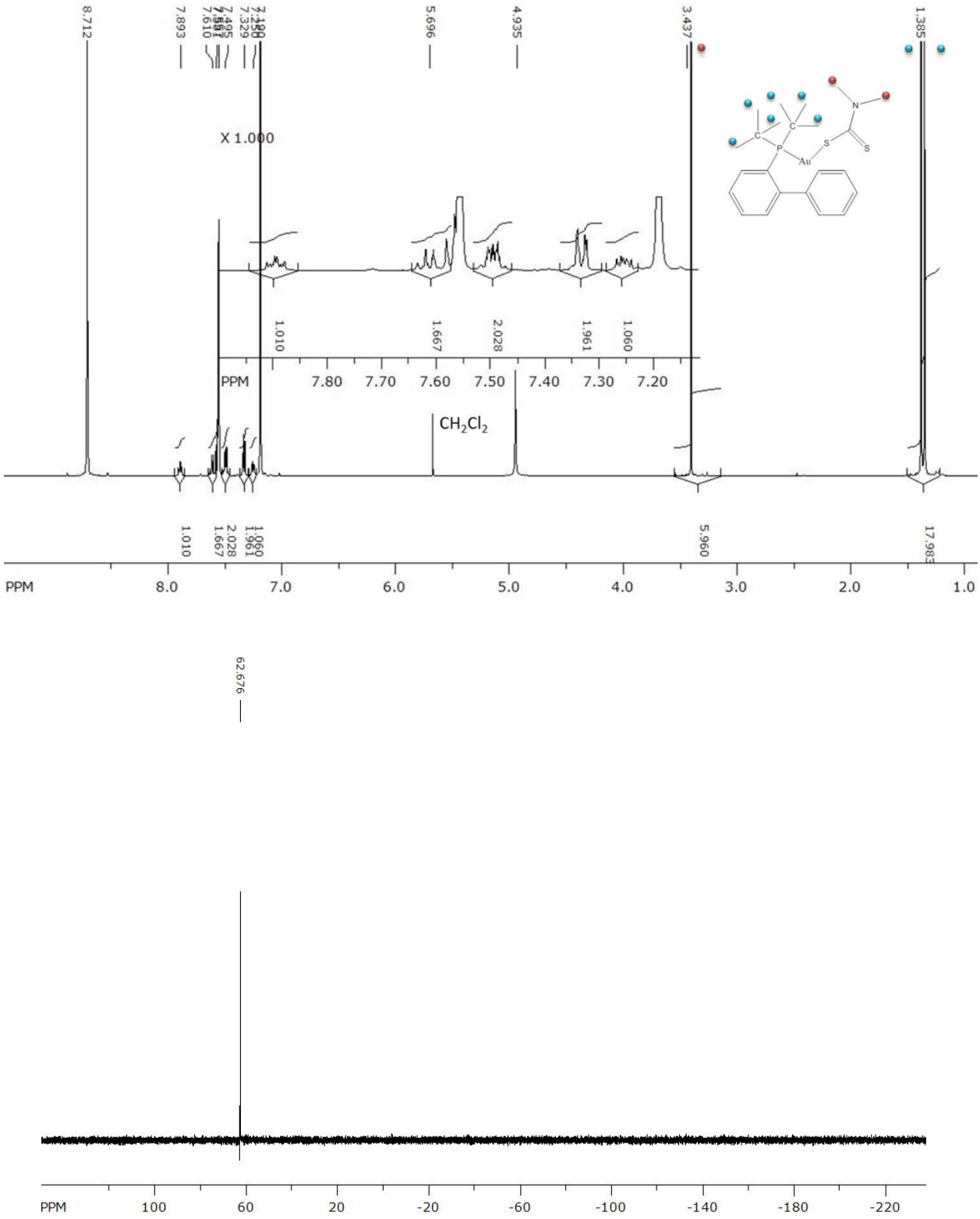

Figure S1. ^{1}H NMR (top) and ^{31}P NMR (bottom) spectra of **1** in pyridine-d^{5}.

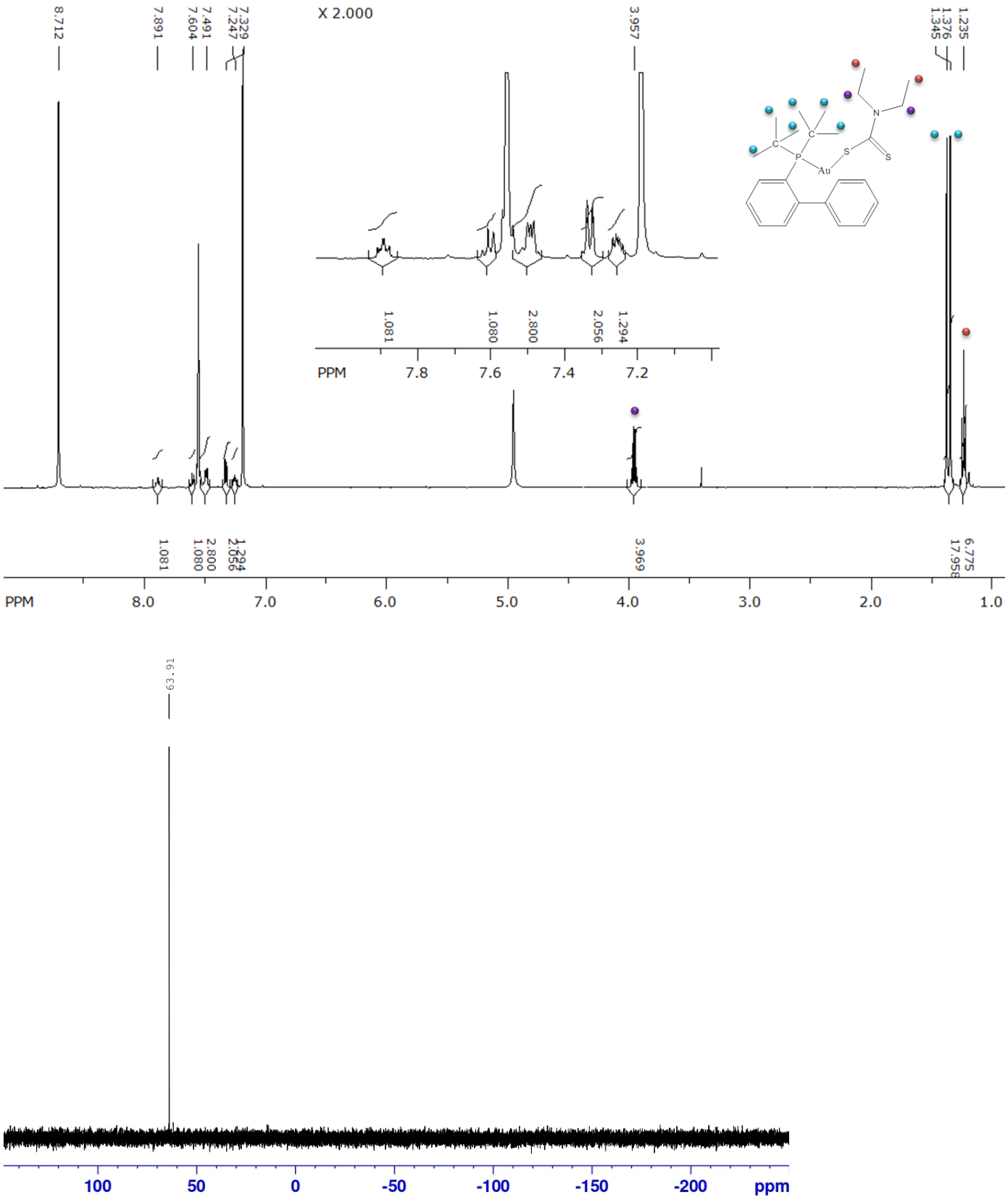

Figure S2. ^{1}H NMR (top) and ^{31}P NMR (bottom) spectra of **2** in pyridine-d^{5}.

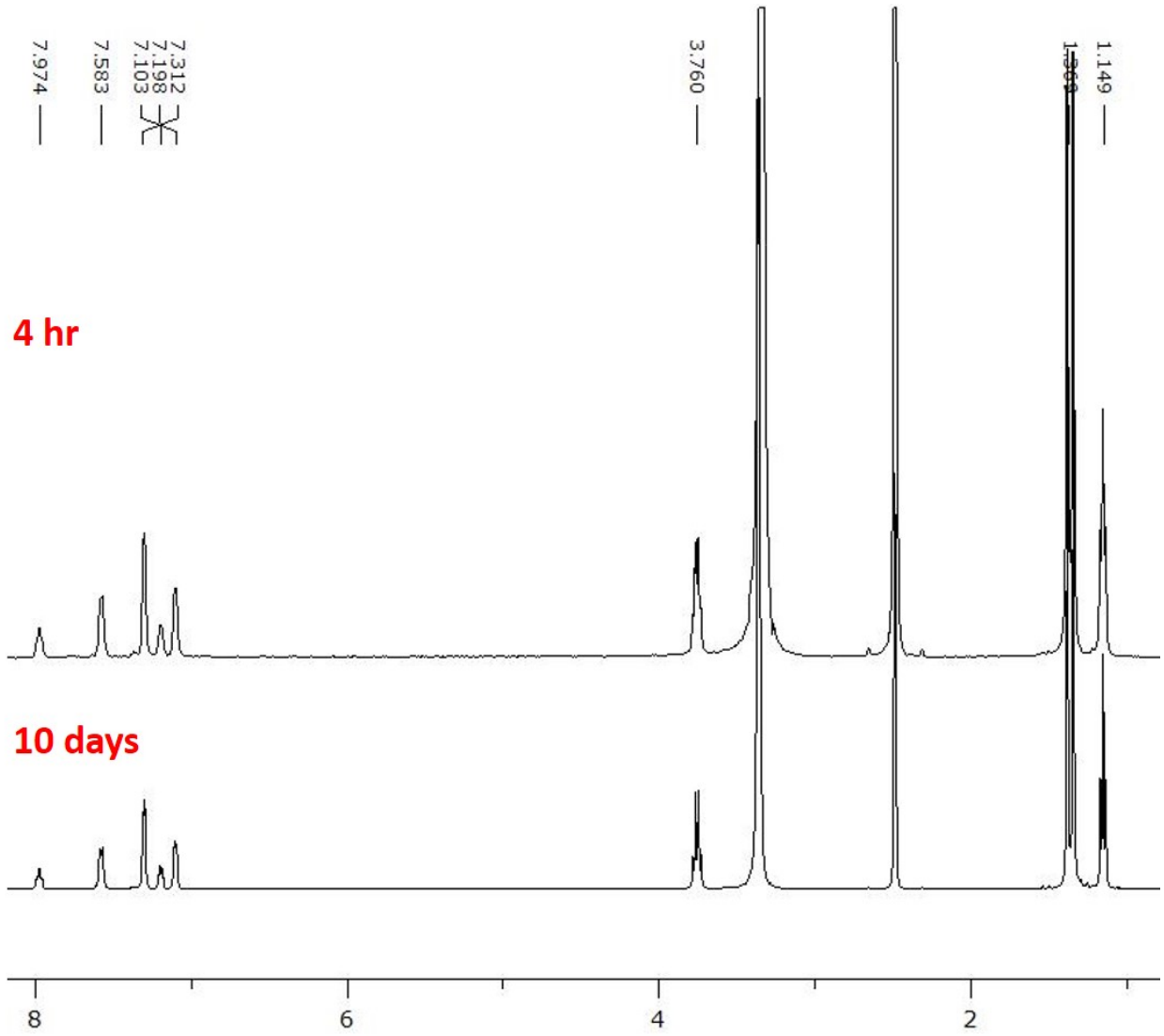

Figure S3. ^{1}H NMR spectra of **2** in DMSO-d^{6} immediately after dissolution and 10 d after dissolution.

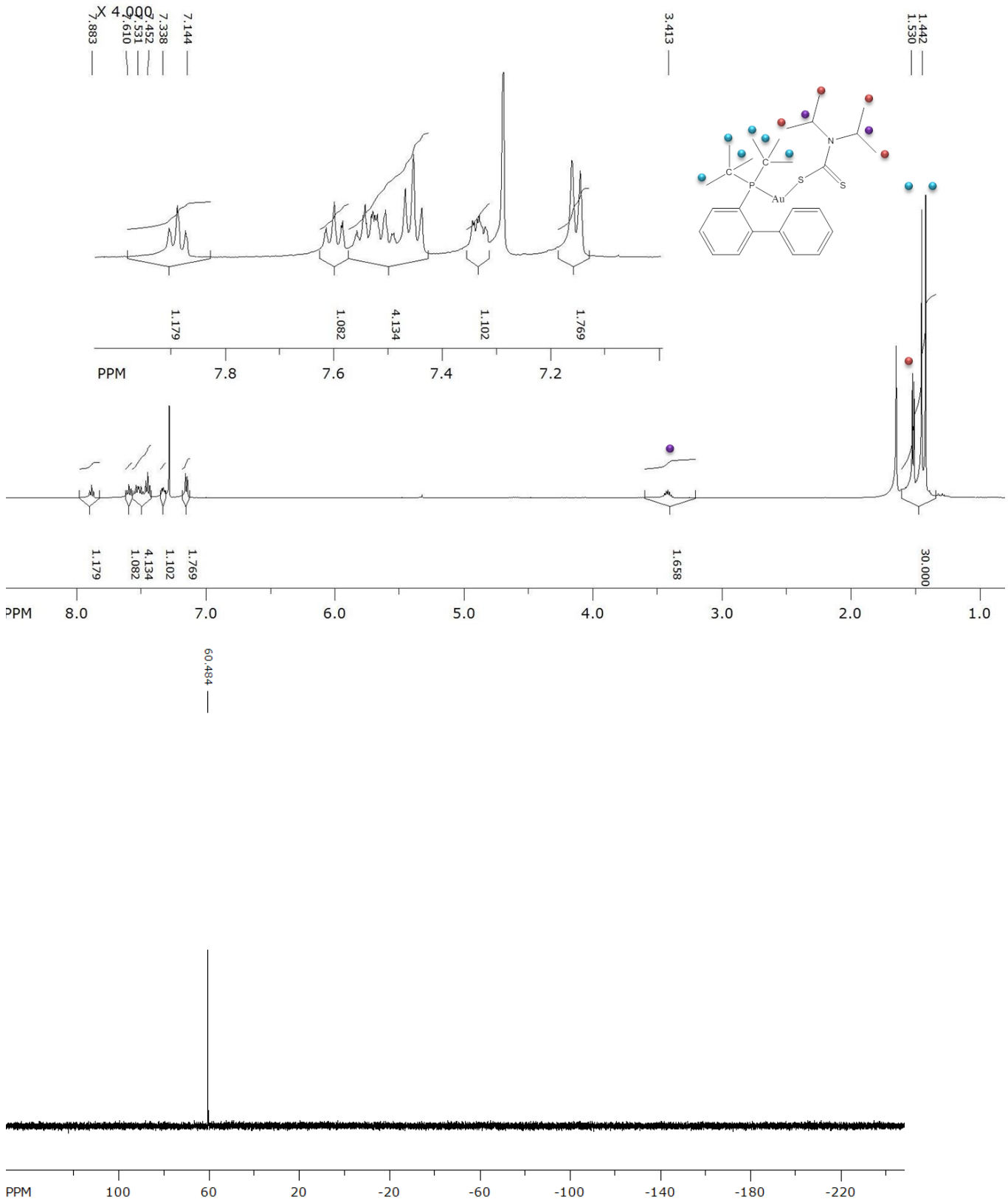

Figure S4. ^{1}H NMR (top) and ^{31}P NMR (bottom) spectra of **3** in $CDCl_3$ immediately after dissolution.

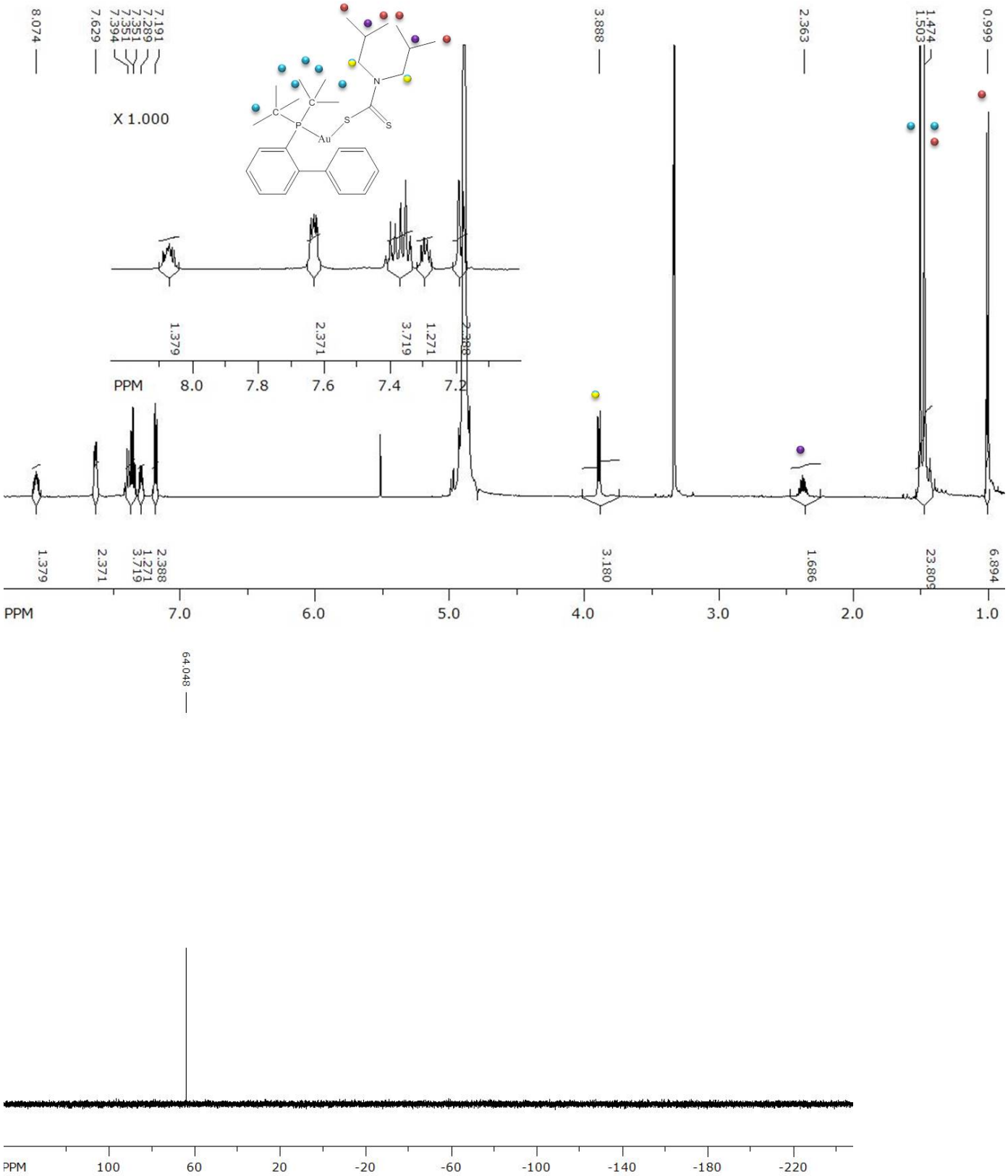

Figure S5. ^{1}H NMR (top) and ^{31}P NMR (bottom) spectra of **4** in methanol-d^{4} immediately after dissolution.

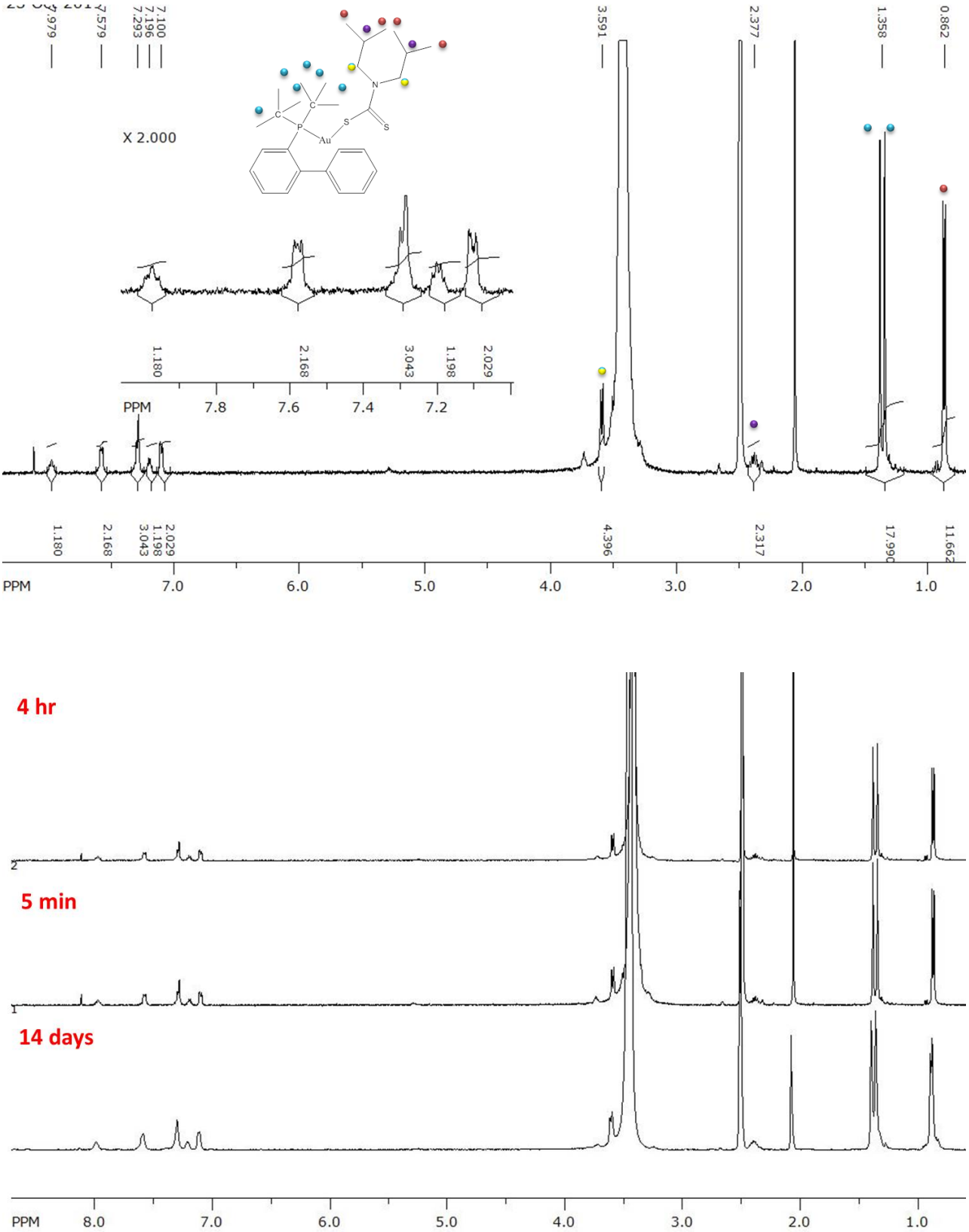

Figure S6. ^{1}H NMR spectra of **4** in DMSO-d^{6} immediately after dissolution (top) and 5 min, 4 h and 14 d after dissolution (bottom).

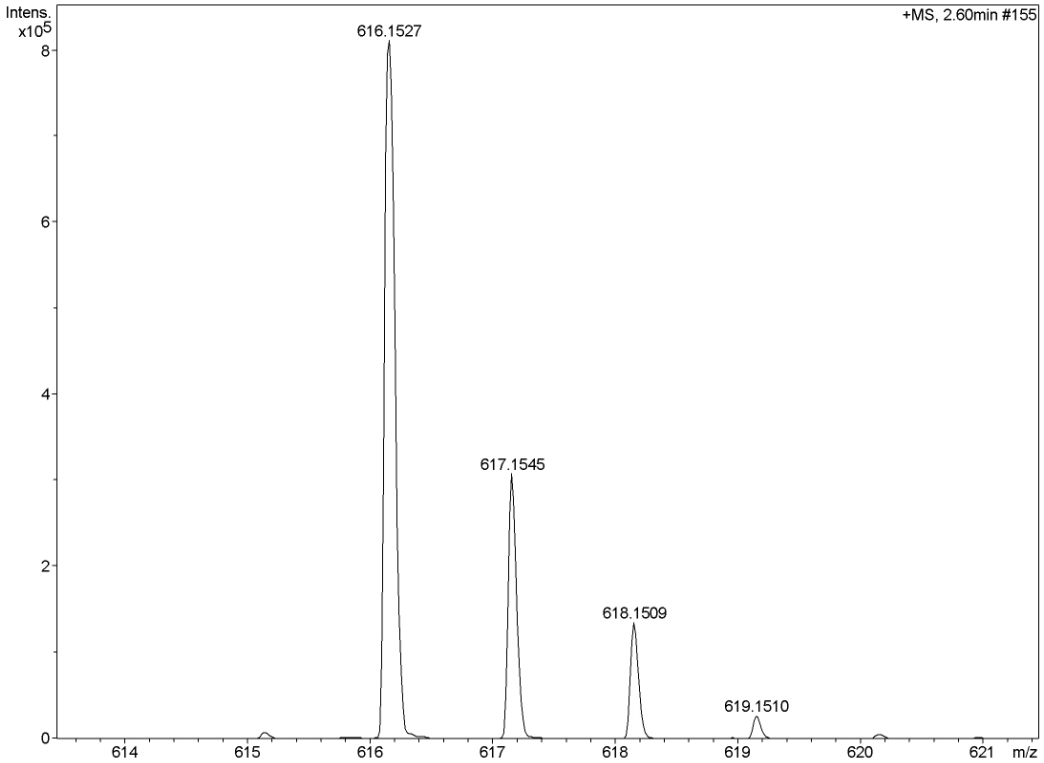

Figure S7. High resolution EI-MS spectrum of **1**.

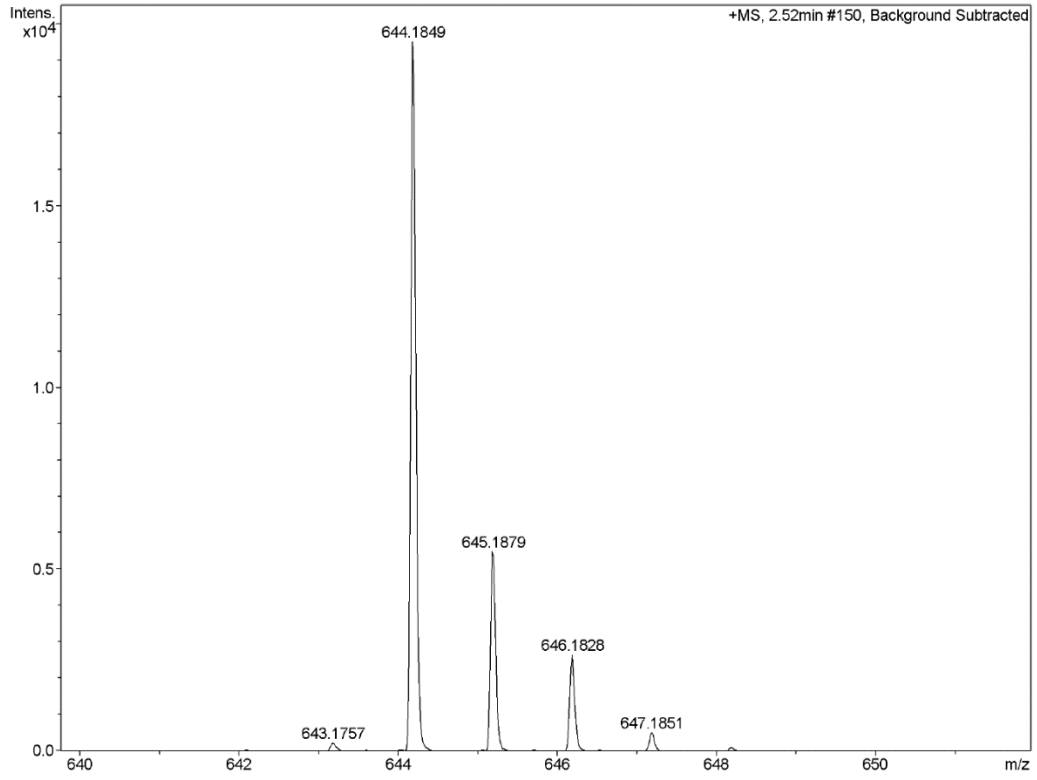

Figure S8. High resolution EI-MS spectrum of **2**.

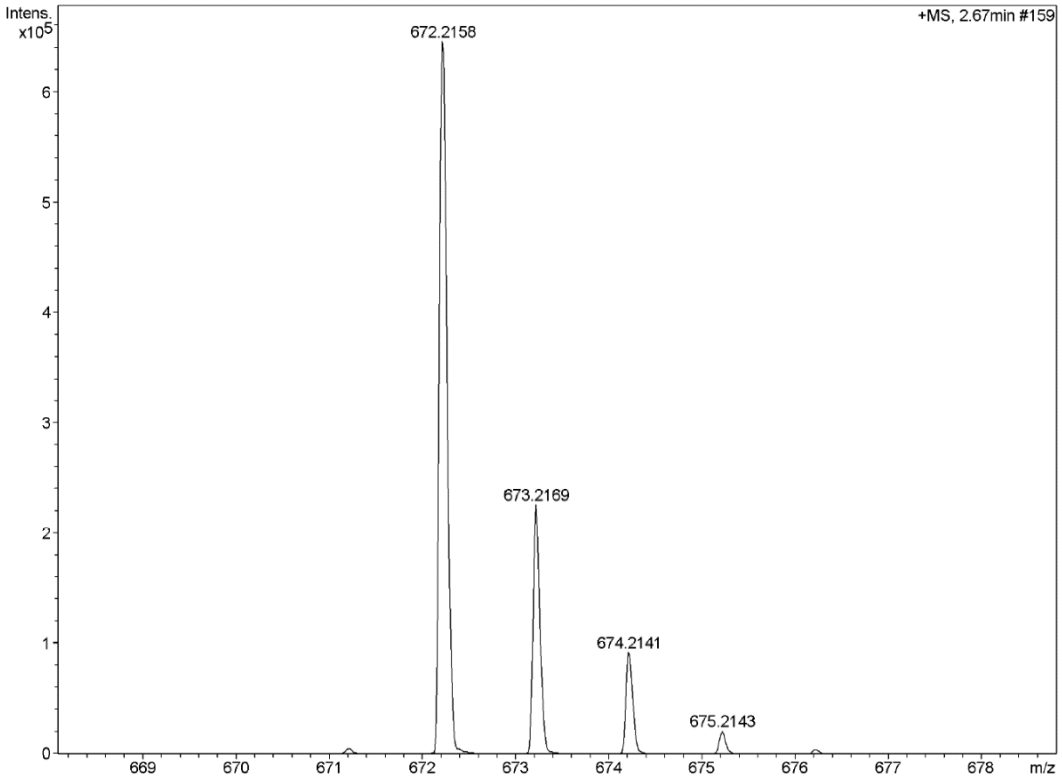

Figure S9. High resolution EI-MS spectrum of **3**.

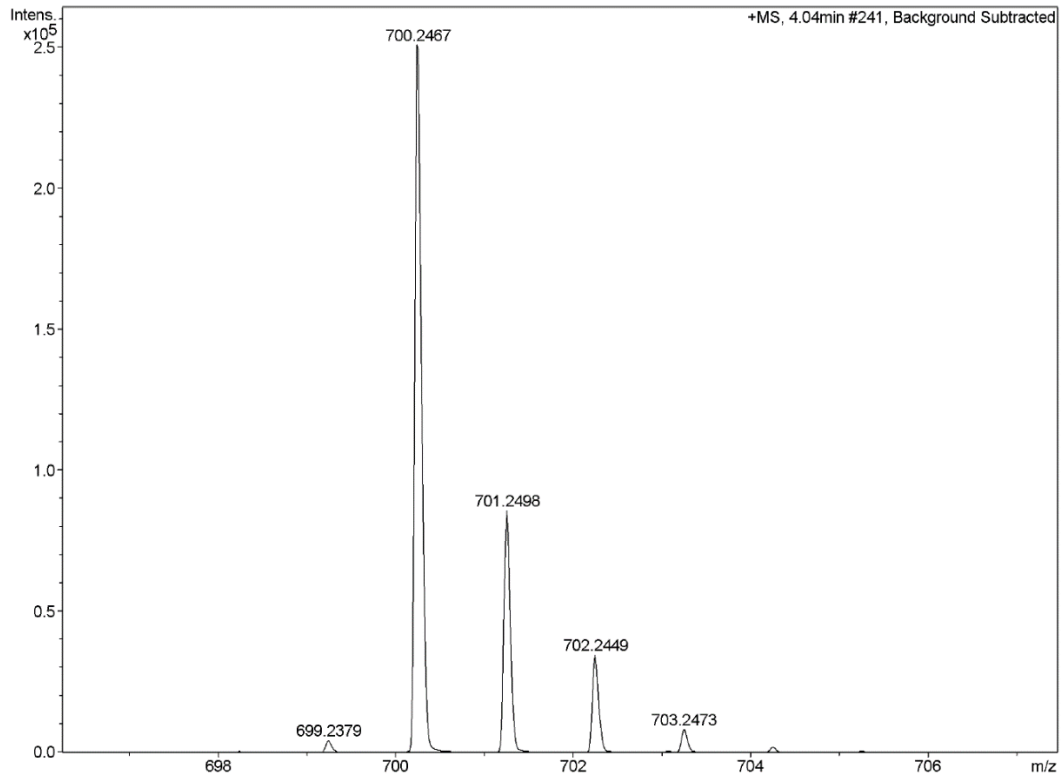

Figure S10. High resolution EI-MS spectrum of **4**.

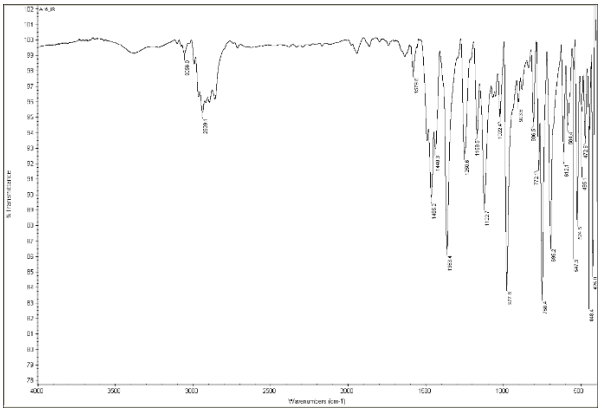

[^{t}Bu$_2$Ph$_2$PAu(S$_2$CNMe$_2$)] (**1**)

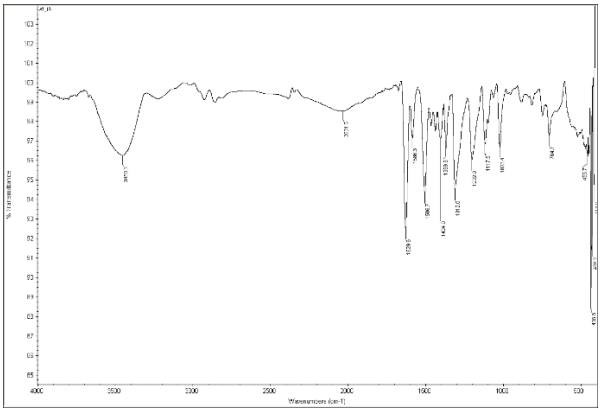

[^{t}Bu$_2$Ph$_2$PAu(S$_2$CNEt$_2$)] (**2**)

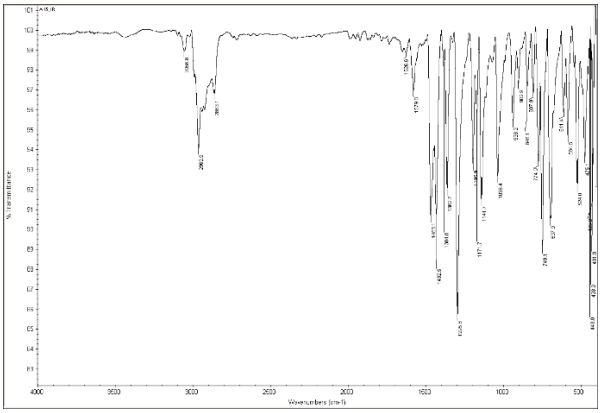

[^{t}Bu$_2$Ph$_2$PAu(S$_2$CN^{i}Pr$_2$)] (**3**)

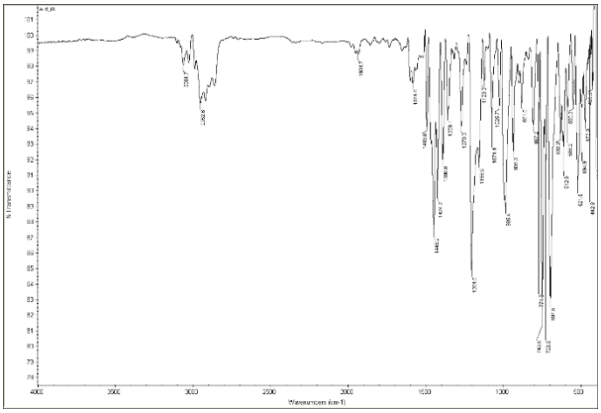

[^{t}Bu$_2$Ph$_2$PAu(S$_2$CN^{i}Bu$_2$)] (**4**)

Figure S11. FT-IR spectra of **1**-**4**.

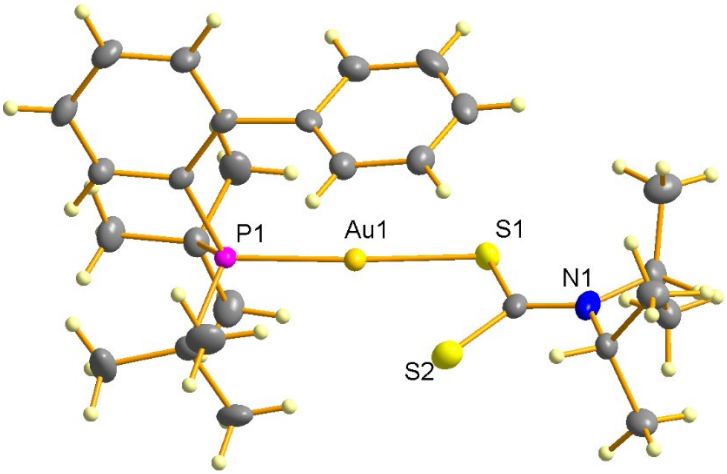

Figure S12. Molecular structure of **4**. Non-H atoms are represented by thermal ellipsoids of 50% probability levels.

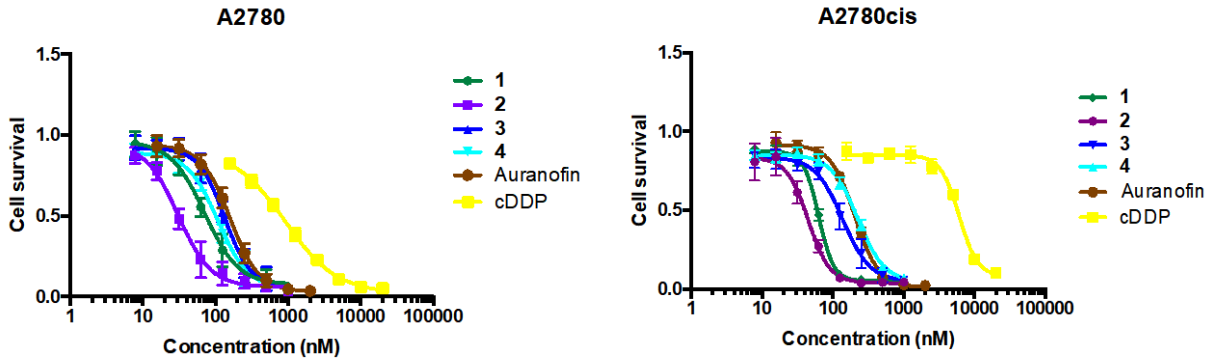

Figure S13. Concentration-effect curves of **1-4**, auranofin and cDDP in the in the human ovarian carcinoma cell lines A2780 and A2780cis obtained by the MTT assay using exposure times of 72 h.

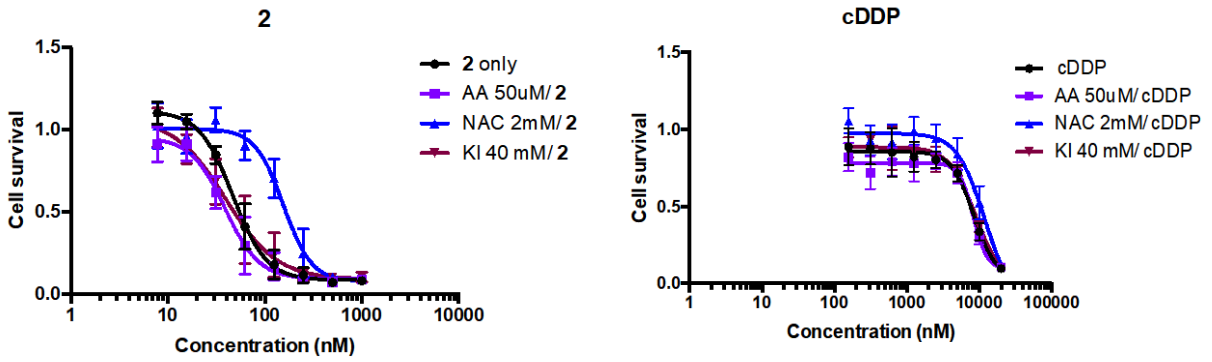

Figure S14. Concentration-effect curves of **2** and cDDP in the human ovarian carcinoma cell line A2780 obtained by the MTT assay using exposure times of 24 h in presence or absence of antioxidants (AA – ascorbic acid, NAC – *N*-acetyl cysteine, KI – potassium iodide).

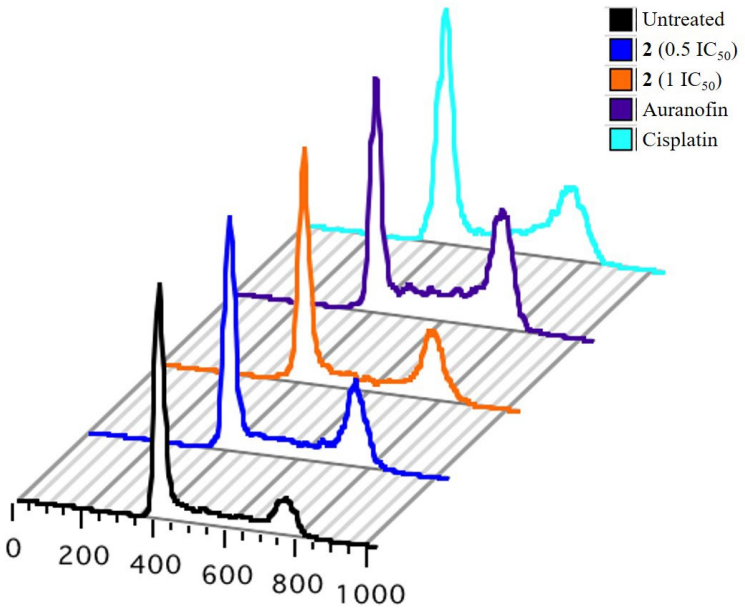

Figure S15. Cell cycle analysis of A2780 cells treated with **2**, auranofin and cDDP for 24 h.